# RESPONSE TO LOAD FOR FOUR DIFFERENT TYPES OF BORED PILES

Bengt H. Fellenius[1)] and Mario Terceros H.[2)]

[1)] Consulting Engineer, 2475 Rothesay Ave., Sidney, BC, Canada, V8L 2B9. <Bengt@Fellenius.net>
[2)] President, Incotec SRL, Santa Cruz, Bolivia. <math@incotec.cc>

## ABSTRACT

Four strain-gage instrumented bored piles were constructed in a sedimentary, dense to very dense, fine to medium sand in Santa Cruz, Bolivia. Two of the test piles were the normally used bored pile constructed with bentonite slurry and two piles were Bauer Full Displacement Pile (FDP). One of each pair was equipped with the Expander Body, an inflatable steel cylinder that on pressure-grouting provides an enlarged pile toe. Head-down static loading test were performed on three of the piles and a bidirectional test was performed on the fourth pile, a standard pile with Expander Body and a bidirectional cell placed immediately above the EB. The latter pile was tested in 3 phases. First by activating the cell, second, by a head-down test, and, third, by a repeat bidirectional cell test. The static loading tests proved the shaft resistance of the FDP pile to be about twice that of the standard bored pile and that the Expander Body more than doubled the toe stiffness. The strain-gage records showed that the standard bored piles had multiple bulges and neckings, which affected the evaluation of the axial stiffness and load distribution of the piles. The testing programme was used for a prediction event with 60 persons, ahead of the tests, submitting predictions of the load-movement curves for the test piles and also a capacity appraised from the curves.

## 1. INTRODUCTION

On April 23 - 26, 2013, the First International Conference and Seminar on Deep Foundations was held in Santa Cruz, Bolivia under the auspices of INCOTEC SRL, the UAGRM University, and the Bolivian Association of Civil Engineers and Chamber of Construction. To coincide with the conference, a research study on construction and static and dynamic testing of four instrumented bored piles was undertaken. To "add spice" to the conference, a prediction event was organized on the test programme. This paper presents the soil conditions at the site, the type and construction of the test piles, the outcome of the prediction event, and the results of the static tests.

## 2. SOIL CONDITIONS

Geotechnical studies comprising SPT and CPT tests with routine laboratory analysis were performed on recovered soil samples. Three SPT boreholes were put down at three of the locations of Pile TP1, TP2, and TP3, at 5.0 m distance from each other. The SPT procedure consisted of manual hoisting of the weight by three crew members pulling on ropes over a pulley supported by a tripod and letting the weight fall by gravity. The groundwater table lies at 3.5 m depth.

Figure 1 shows diagrams of the SPT N-indices and the distribution of water content in the three boreholes. The SPT-indices show the soil density to be compact. The average water content is about 15 %, plus-minus a few percent.

When the field study was planned, it was expected that the site information would include also a couple of CPTU soundings. However, the CPTU equipment did not become available until well after the event. Obviously, the participants in the prediction event did not have the benefit of the CPTU data. Three CPTU soundings were performed in between the four test piles. The three gave very similar results. Figure 2 shows the CPTU diagrams from CPT-1; measured cone stress, sleeve friction, pore pressure on the cone shoulder (U2), and calculated friction ratio.

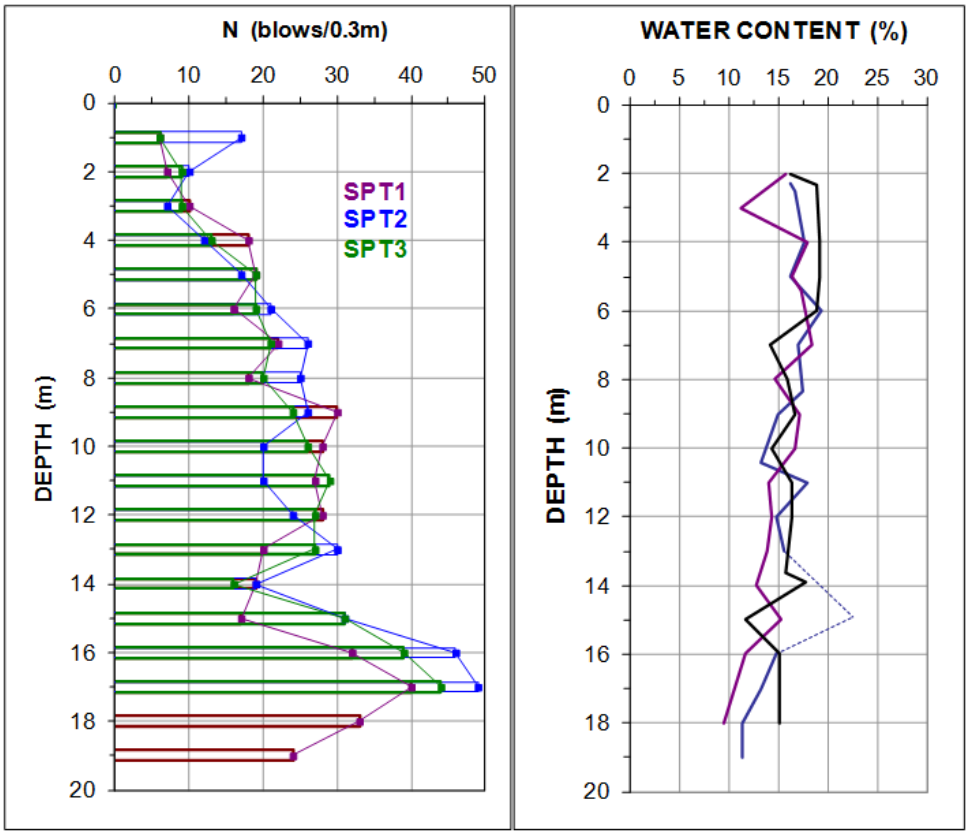


Fig. 1 SPT N-indices and Water Contents

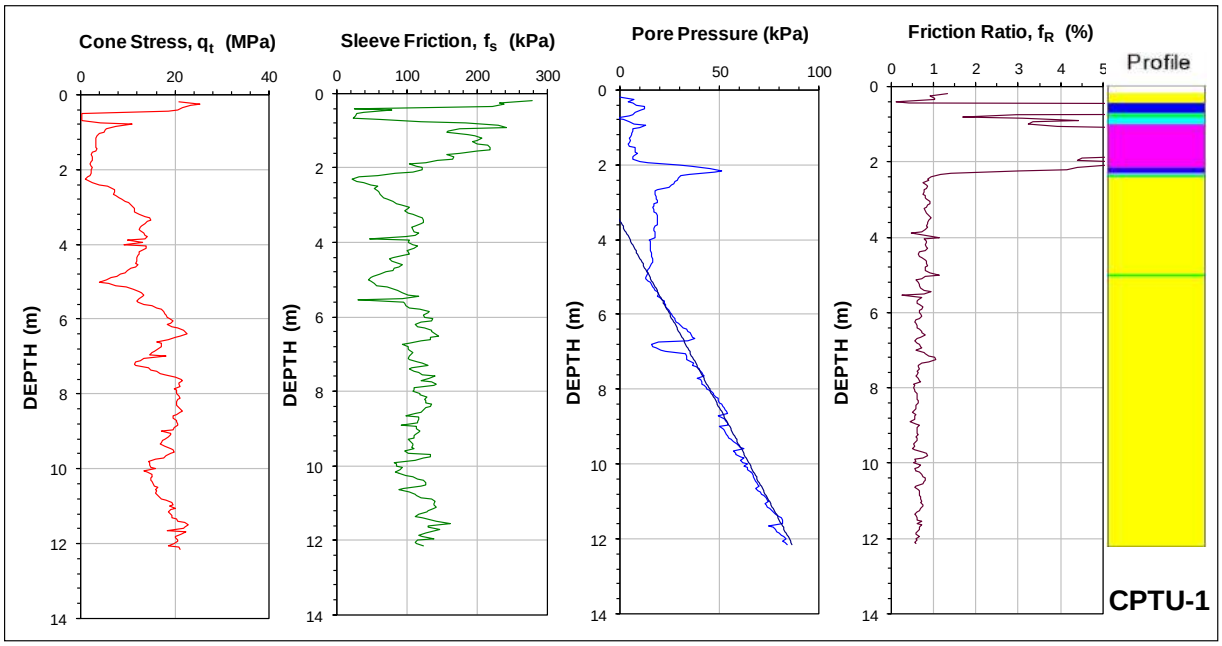


Fig. 2 CPTU diagrams

Figure 3 shows the grain size distributions obtained in the three boreholes, with the dominant fraction to be fine to medium sand with trace fines. Between 14 and 16 m depth, a zone of clay and clayey sand was encountered.

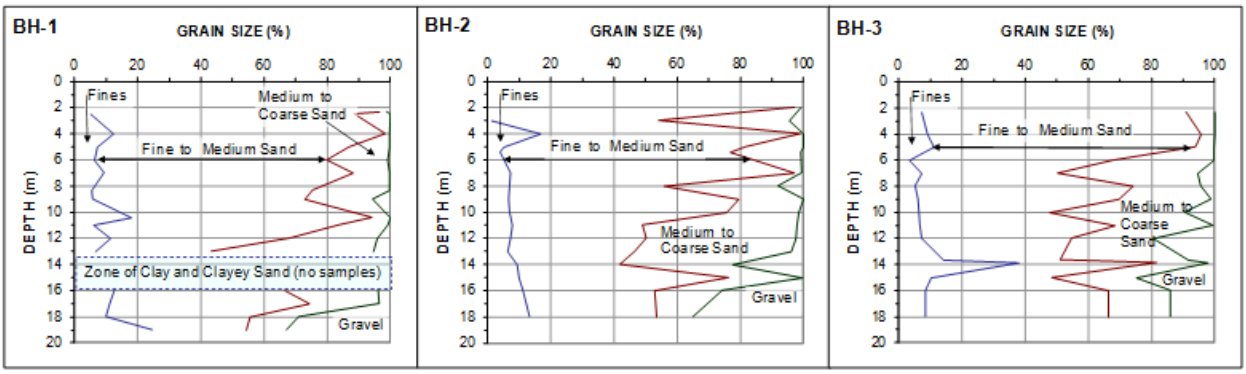


Fig. 3 Grain size distributions

## 3. PILE CONSTRUCTION DETAILS

The test piles were bored piles described as follows.

**TP1**: a nominally 400-mm diameter pile, 17.5-m length, bored under bentonite ("standard pile").

**TP2**: a nominally 360-mm diameter pile, 11.6-m length, built as a FDP (Full Displacement Pile) which is constructed without removing any soil (but for nearest the ground surface on starting the pile).

**TP3**: a nominally 360-mm diameter pile, 9.6-m length, built as a FDP (Full Displacement Pile) and with a 600-mm diameter Expander Body, EB (Broms and Nord 1985, Massarsch and Wetterling 1993, Terceros et al. 1995), placed at the pile toe.

**TP4**: a nominally 450-mm diameter pile, 17.5-m length, bored under bentonite and with a 600-mm diameter Expander Body, EB, placed at the pile toe and with a bidirectional-cell (Osterberg cell) above the EB.

Figure 4 shows a plan of the borehole and test pile locations in plan and the locations of the reference beam supports and the reaction piles, RP1 through RP10.

Figure 5 shows a vertical view of the test piles and the instrumentation depths with depth to the vibrating-wire strain-gage levels.

The concrete was designed to have 30 MPa cylinder strength. The reinforcement cage consisted of six 12 mm bars for the piles without EB (TP1 and TP2) and of six 16 mm bars for the piles with EB (TP3 and TP4). For all four piles, the reinforcement cage had a 6-mm spiral with a 250-mm pitch along the full length but for the first 1.5 m below the pile head where the pitch was 50 mm. For Piles TP1 - TP3, the reinforcing cage was placed along the full length of the piles.

The EB units (Piles TP3 and TP4) were expanded using pressure grouting immediately after the pile had been concreted. To offset shortening of the height of the expander, which occurs during expansion, also the soil below the EB was pressure grouted. To further increase soil stiffness and strength, pressure grouting was implemented at the bottom of the EB. The expansion (inflation) significantly increases the earth stress against the EB. Figure 6 shows the EB grouting pressure and grout volume measured at the grouting pump during the expansion of the two EB units. The pressure-grouting curve of Pile TP3 shows a normal development for an EB in loose to compact soil. The EB in Pile TP4 required a slightly larger grouting pressure.

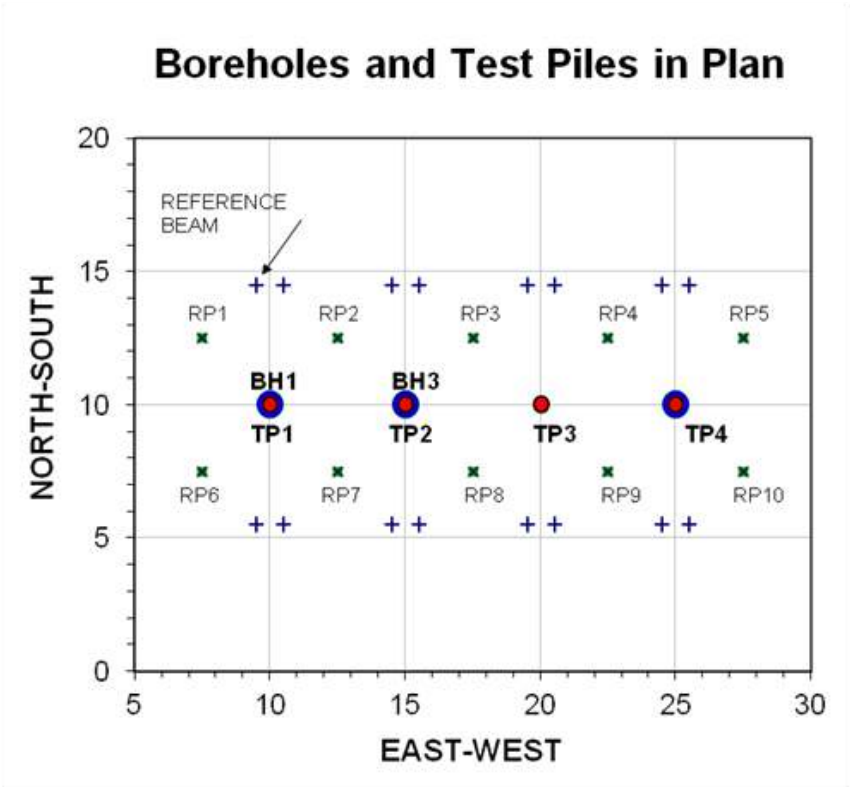


Fig. 4 Plan view of the test site

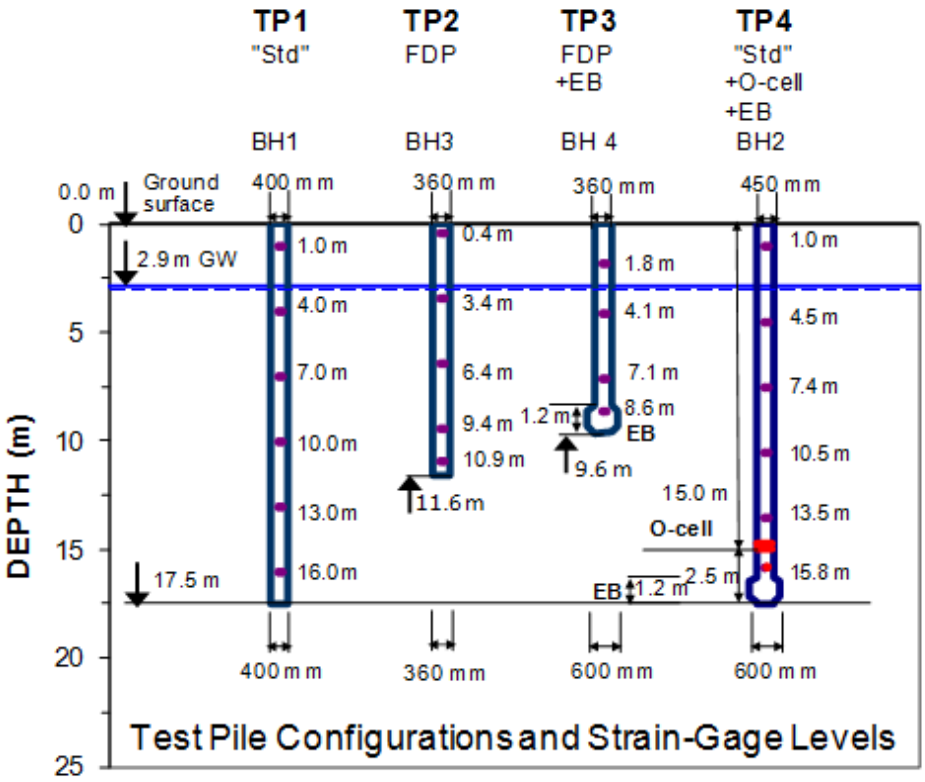


Fig. 5 Vertical view of the test site

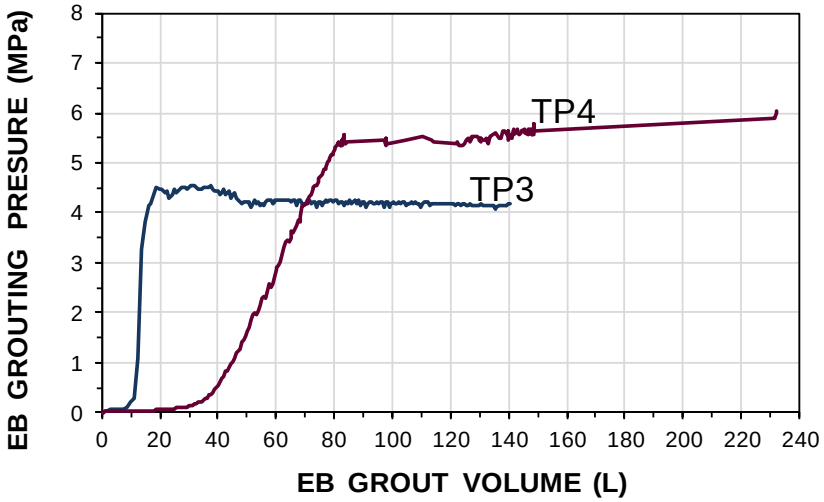


Fig. 6 Expander Body grout pressure and grout volume for Pile T3 and TP4

Construction of test piles TP1, TP2, and TP3 were completed on March 8, 11, and 13, respectively, and the construction of Pile TP4 was completed on March 18, 2013. The details of each pile are:

**Test Pile TP1**, a "standard" pile, constructed per the methods normally applied in Bolivia, as follows: A hole was drilled using a rotating cutting tool with a 400 mm helix attached to the end of a drill pipe (kelly). The drilling was pursued with continuous pumping of bentonite slurry up to a swivel entry at the top of the drill pipe, down through the drill pipe, and to the cutting tool. As the drill advanced into the ground, the cutting tool mixed the soil with the slurry, and the continuous injection of slurry sent the mix up to the ground surface along the pipe. The mix then flowed by gravity in channels on the ground to a collection pit, where it was desanded and pumped back to the pile. When the drill pipe had reached the desired depth, circulation of desanded slurry was continued until the sand content in the mix at the ground was deemed acceptably low. The acceptance criterion for viscosity was 40 seconds for a litre of slurry to flow out of a Marsh funnel and no more than 2 % of sand content. The drill pipe was then withdrawn and the reinforcing cage was lowered into the slurry. Then, a tremie pipe is inserted through the slurry to the pile toe to replace the slurry with concrete in a regular tremie process.

**Test Pile TP2**, an FDP pile constructed to 11.6 m depth without removing any soil. The equipment consisted of a 360-mm maximum O.D. pipe (displacement body) with a 25-mm wall attached to an auger length. Rotating the auger pulls down the displacement body. When the desired depth had been reached, concrete was pumped through the displacement body auger tip during the withdrawal of the displacement body. Thereafter, the reinforcement cage was lowered into the concrete to the pile toe.

**Test Pile TP3** a standard pile similar to TP2, but for being supplied with an Expander Body at the pile toe (installed attached to the end of the reinforcing cage). The EB was expanded after the shaft was concreted.

**Test Pile TP4** a standard pile constructed with a 450-mm diameter helical cutting tool and supplied with an Expander Body at the pile toe. A 450 mm diameter bidirectional-cell (Osterberg cell) was placed with its bottom plate at 15.0 m depth.

## 4. RESULTS OF THERMAL PROFILING

The actual pile diameter of a bored pile will always deviate from the nominal diameter. The actual diameter of the test piles was estimated two ways. One was by measuring the concrete volume, which

gave an average pile diameter. The second was by means of thermal wires installed on the reinforcing cage. The monitoring of the rate of cooling of the pile was used to determine the diameter distribution, as for example described by Mullins (2010). Figure 7 shows the results of the measurements. For Pile TP1, it would seem that the average diameter determined from the concrete volume agreed with the thermal profiling. However, there is little or no agreement between the two methods for the other three test piles. Qualitatively, however, the thermal profiling also indicated that the as-constructed pile shaft diameters varied for the standard piles.

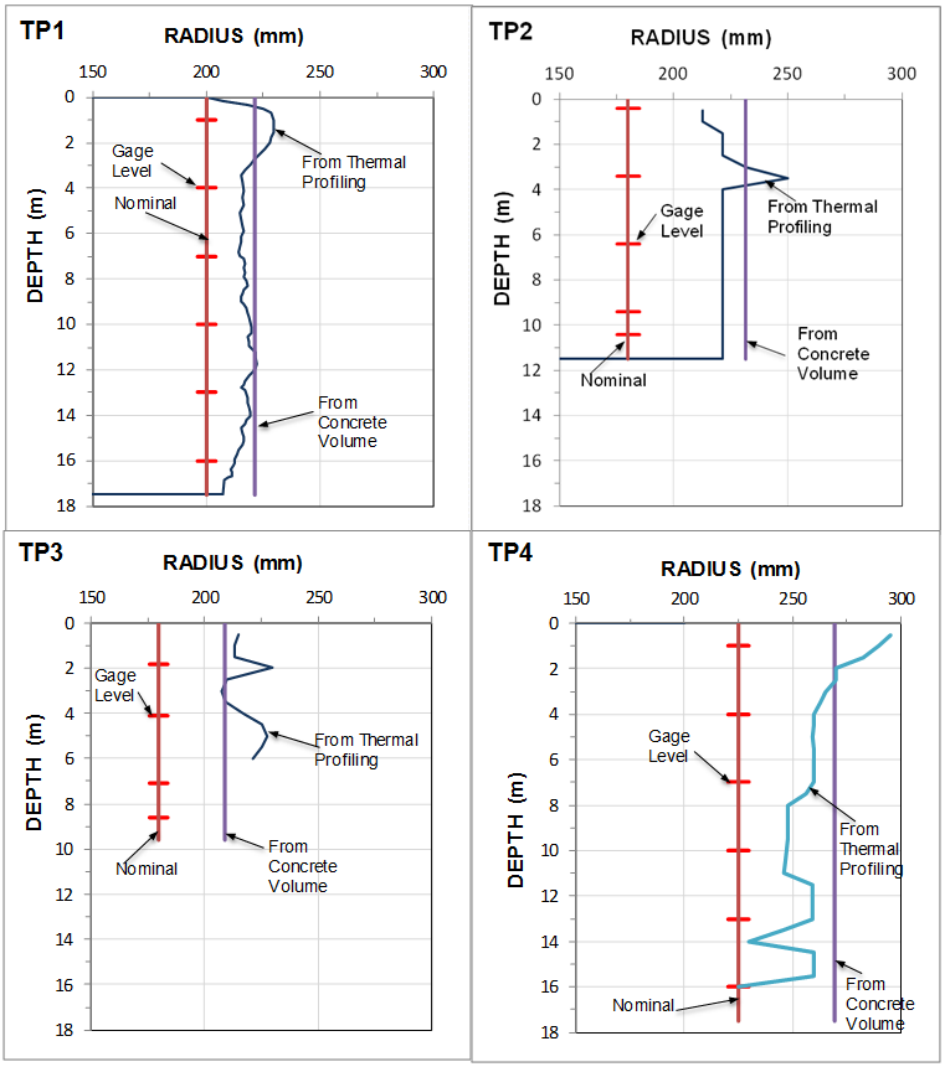


Fig. 7 Nominal pile radii and radii evaluated from thermal profiling and from average volume of concrete. The strain-gage levels are indicated for reference.

## 5. RESULTS OF THE STATIC LOADING TESTS—LOAD-MOVEMENT DATA

The static loading tests on Piles TP1 - TP3 were carried out as incremental maintained-load head-down tests with equal load increments of nominally 100 kN applied every 10 minutes. The loads were applied by means of a manometer-controlled hydraulic jack and the applied load to the pile was measured with a separate load cell. Pile TP4 was tested in three phases. Phase 1 was a bidirectional cell test with equal load increments of 75 kN applied every 9 minutes. Phase 2 was a subsequent head-down test with the cell open and draining and the test followed the same procedure as for Pile TP1 through TP4. Phase 3 was a repeat bidirectional cell test with equal load increments of 75 kN applied every 9 minutes. The load-movements recorded during the tests on Pile TP1 through TP3 and Pile TP4 Phase 1 are shown in Figure 8.

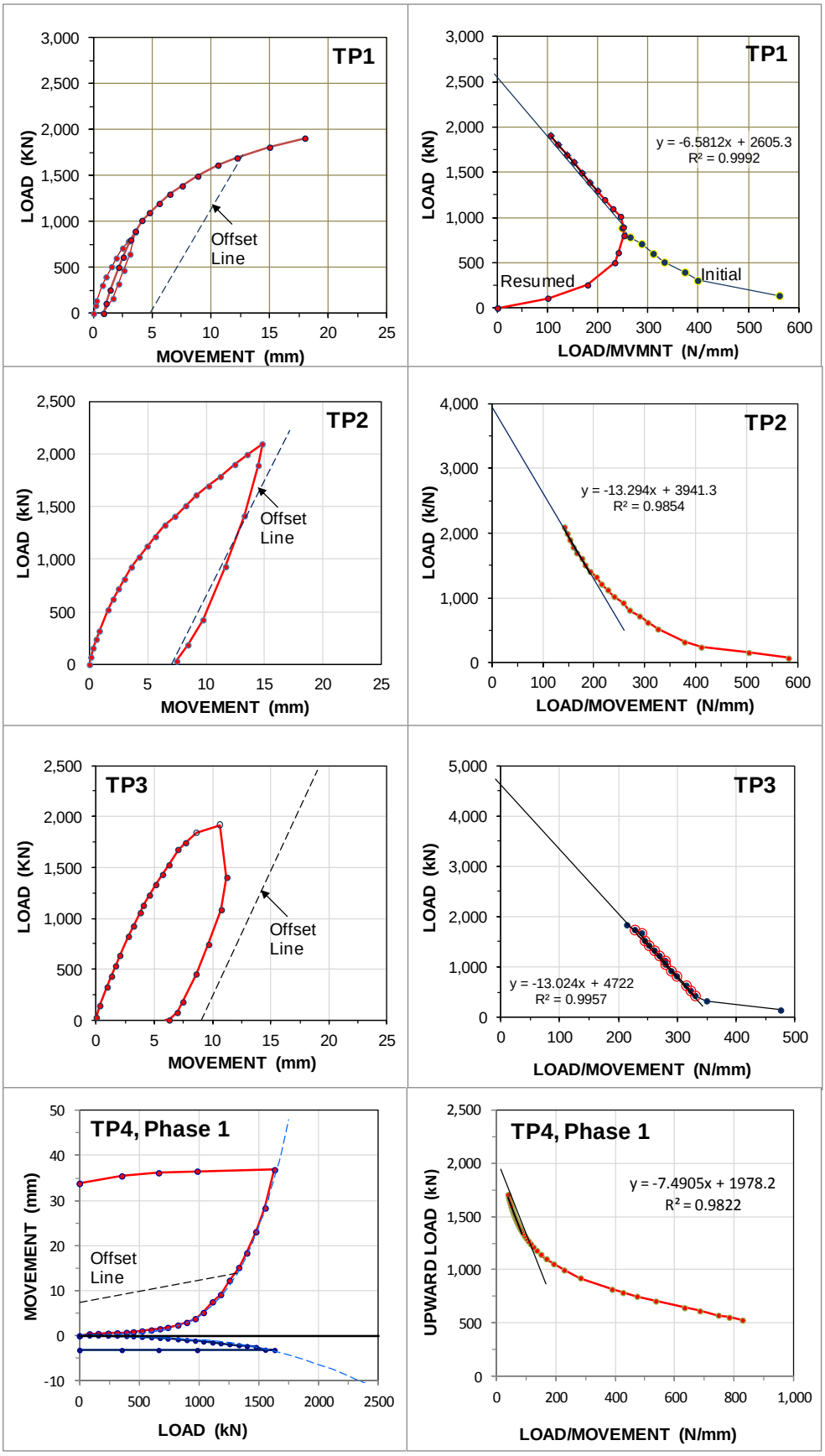


Fig. 8 TP1-TP4 Load-movement curves and Decourt constructions

**Pile TP1**. TheTP1 test started on April 15, 2013, 38 days after construction. At the applied load of about 900 kN, a hydraulic hose between the pump and the jack sprung a leak and the pile had to be unloaded. After repair, the test was resumed. At the load of 1,908 kN, the pile broke at the ground surface and the test was terminated. The straight dashed line in Figure 9A is the offset limit line, which intersection with the pile head load-movement curve is generally considered to be a lower-bound value of the capacity of the pile, occurring for Pile TP1 at 1,700 kN. The Offset Limit Line was calculated using a pile modulus, E, of 25 GPa and the nominal cross section for the shaft and the pile toe—the pile toe diameter of the EB was used for Pile TP3. The diagram to the right of the load-movement diagram shows the construction of the pile capacity per the Decourt Extrapolation (Decourt 2008), which is the load that the load-movement curve, if continuing in a hyperbolic shape, would asymptotically approach at very large pile head movements. The Decourt extrapolated capacity for Pile TP1 is 2,600 kN). It is clear that the pile was approaching soil failure when it broke. The pile capacity can be considered to be about 2,000 kN.

It is interesting to see that, before the load applied in the resumed test had reached the previously applied load, the first part of the Decourt construction for the reloading records is very different from the construction using the initial loading records.

**Pile TP2**. The TP2 test started April 16, 36 days after construction. At the applied load of 2,100 kN, the hydraulic jack selected for the test reached its limit and the test had to be terminated. Extrapolation of the curve suggests that the curve would have intersected the Offset Limit Line at about 2,300 kN. The Decourt extrapolation indicates 3,900 kN. Had the test continued, it is probable that the capacity estimated from the load-movement curve would have been about 2,500 kN.

**Pile TP3**. The TP3 test started April 17, 34 days after construction. At the applied load of 1,800 kN, the pile head started showing cracks, the jack to tilt, and the pile head to deform. After two additional load increments, the pile broke right at the pile head. Extrapolation to an Offset Limit Load would be too uncertain to attempt. The Decourt construction indicates 4,700 kN.

**Pile TP4 Phase 1**. The TP4, Phase 1 test started April 17, 32 days after construction. When the cell load was 1,630 kN, the downward movement was 3 mm for the lower 2.5 m length of the pile (dominated by the 1.2 m long EB). The movement upward of the upper length was then 37 mm suggesting that the capacity of the upward length had been exceeded. The cell was then unloaded. There was no rebound of the lower length. After unloading, the opening between the cell plates was 37 mm. The upper cell plate rebounded (downward) 3.0 mm, which was twice the 1.3 mm maximum shortening of the pile. The offset limit construction for the upward length (shaft resistance only) intersected the curve at 1,300 kN. The Decourt extrapolation is 1,980 kN. The shaft capacity, is considered to be about 1,500 kN for the 15.0 mm long pile shaft above the cell. The response of the lower length with the EB is very stiff; the slope of the load-movement curve is 5 GN/m.

**Pile TP4 Phase 2**. Pile TP4 Phase 2 proceeded immediately after Phase 1. The procedure was to push the pile head down using a jack placed on the pile head. Loads were measured with a separate load cell. The bidirectional-cell at 15 m depth was kept draining as the upper length was pushed down and the distance between the cell plates reduced. The cell valve was accidentally closed at one point which generated load in the cell and temporarily affected the downward movement of the upper pile. The measured load-movement records are shown in Figure 9A. It is notable that the load to achieve the upward shaft movement is equal to the load to achieve about equal downward shaft movement. This supports the generally accepted fact that ultimate shaft resistance acting in upward direction is equal to shaft resistance acting in downward direction.

**Pile TP4 Phase 3**. Pile TP4 Phase 3 proceeded the day after Phase 2 and consisted of a resumed bidirectional cell test. Figure 9B shows the results. The upward load movement was similar to the Phase 2 response. At the movement equal to the maximum upward movement in Phase 1, the load applied in Phase 2 was the same as the maximum load applied in Phase 1, a repeat confirmation that direction of movement is of no consequence for the shaft shear resistance.

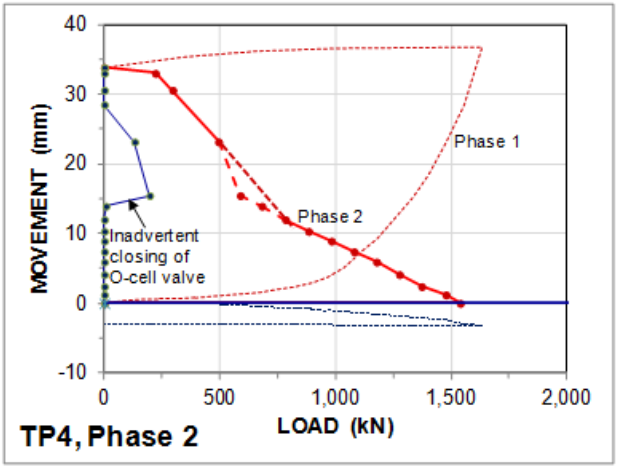


Fig. 9A Load-movement curve from Pile TP4 Phase 2

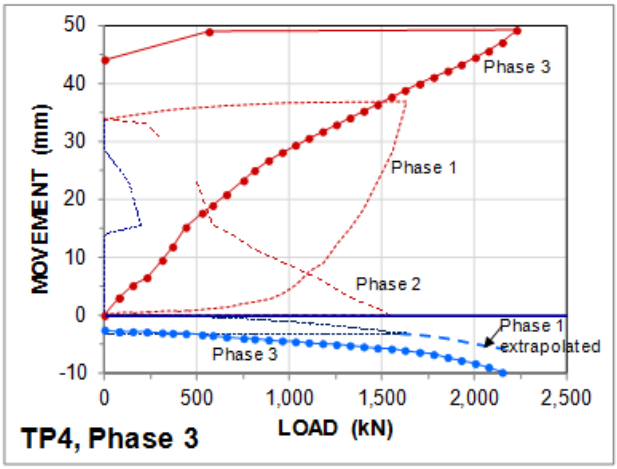


Fig. 9B Load-movement curve from Pile TP4 Phase 3

## 6. RESULTS OF THE STATIC LOADING TESTS PREDICTIONS

Because the timing of the field tests was close to the planned April conference, it was decided to invite the geotechnical community to predict the outcome of the four tests and have the results presented to the conference. Thus, an invitation was disseminated in January and February 2013, soliciting predictions of the pile-head load-movement curve measured in the tests and also to include the capacity determined from the load movement curve and the load distribution along the test pile for an applied load equal to the capacity of the pile. The soliciting letter included the site information presented in Figure 1 and Figures 3 through 5, and a description of the test piles.

A total of 50 predictions was received from 63 individuals in 19 countries and all continents. Most only addressed Pile TP1. Figures 10A through 10D shows a compilation of the submitted load-movement curves and the evaluated capacities. It is pleasant to see that so may actually agreed to submit a prediction despite the limited site information. Only one of the participants had experience from the Bolivian soil and piling conditions. All others can be said to have sent off a shot in the dark using the universal method of guesstimating. Therefore, it is no surprise that the upper and lower boundaries of the load-movement curves and the capacities are wide apart. More surprising, nay extraordinary, is that the range of pile head movements at the evaluated capacities is even wider. Most geotechnical engineers would, we believe, accept an allowable load of half a capacity occurring at a movement of about 15 to 20 mm. But would they be equally willing to accept that same allowable load determined from a capacity that took 50+ mm movement to develop? Indeed, the main outcome of the prediction event is that the geotechnical community has very diffuse definitions of capacity as determined from the results of a static loading test. Few text books, guidelines, codes, and standards, if any, define how to determine the capacity that serves as reference to the proclaimed factors of safety or resistance factors, often with two-decimals precision. We consider this to be a definite weakness in the geotechnical practice.

## 7. STRAIN-GAGE RECORDS AND LOAD DISTRIBUTION

### 7.1 Measurements of Strain before the Static Loading Tests

The first reading of the vibrating wire strain gages— strain and temperature—in each of Piles TP1 through TP3 was taken when the reinforcing cage was ready to be installed into the pile. Readings were then taken after the concrete had been placed and frequently thereafter during the wait period until the start of the static loading test. Figure 11 shows the change of strain recorded at the uppermost and lowest strain-gage level in pile TP1 along with the temperature during the wait period. The temperature, which is plotted against a reverse axis, first rose rapidly due to the hydration of the concrete. After about five days, the temperature stabilized at about 26°C to 28 °C (it will eventually

reduce to the mean annual temperature in the Santa Cruz area, 23°C). Because the pile diameters are small, the temperature rise is small as opposed to that found in other similar studies involving large diameter piles (Fellenius et al. 2009). Moreover, the latter studies showed that the temperature rise (caused by the concrete hydration) reached a peak after about 24 hours and then reduced within the next 5 to 10 days. The trend at the current site was different. It may be that the hydration effect on the temperature is less pronounced for the concrete used in the test piles.

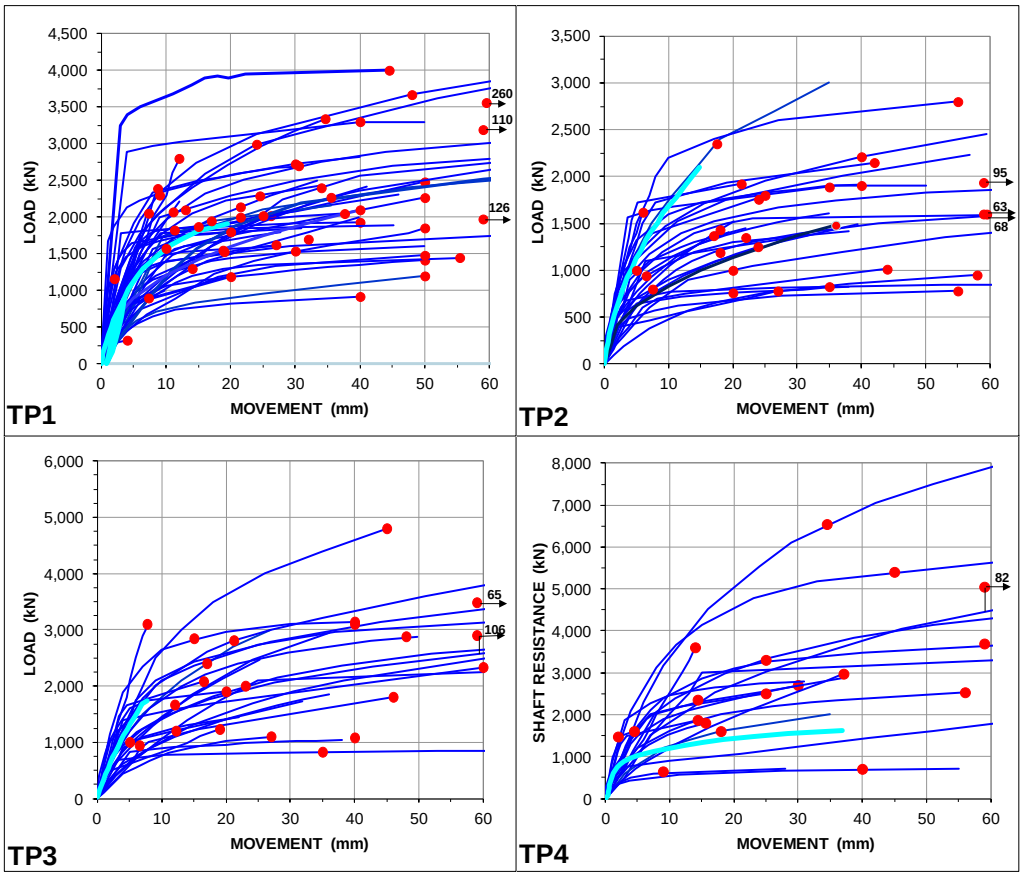


Fig. 10 Piles TP1 - TP4 Capacities and Predicted Load-Movement Curves
Light Blue Curves are from the actual static loading tests

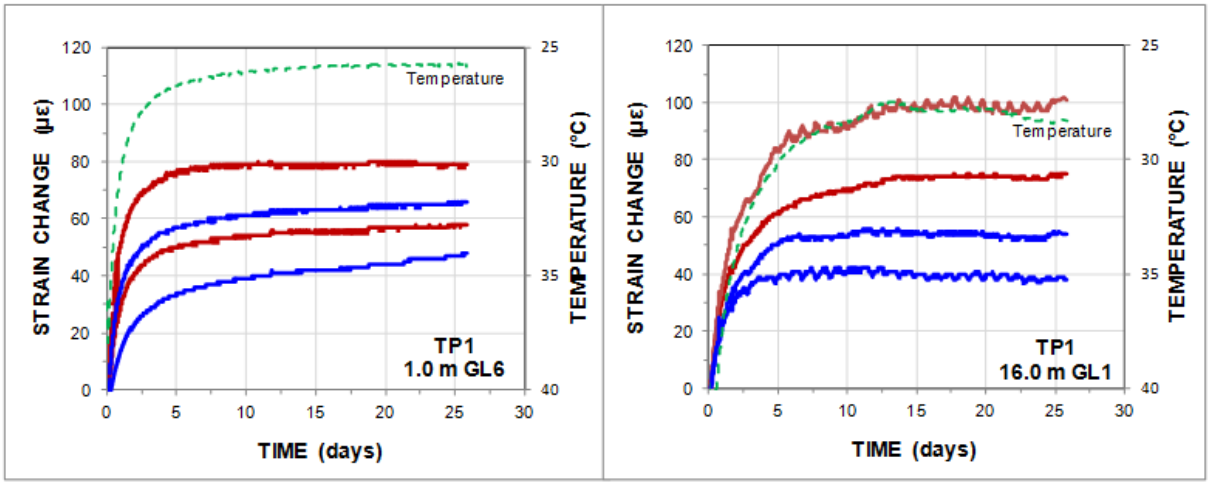


Fig. 11 Pile TP1 Change of strain in the two gage pairs at GL 6 and GL1 (1.0 m and 16.0 m depth) and temperature during the period between construction and start of the static loading test

The development of strain at the other gage levels in piles TP1 through TP3 was similar to that shown in Figure 11, that is, the strain in the pile increased proportionally to the temperature rise and ceased once the temperature had stabilized—within the first week after concrete was placed. The strain change is considered due to the difference in thermal response between the concrete and the steel. The thermal expansion of the concrete was smaller than that of the reinforcing steel, impeding its full expansion, which registered as an increase of compressive strain in the gages. (N.B., the gages themselves are insensitive to temperature changes). Such changes of strain are internal and do not affect forces between the pile and the soil. Therefore, it is concluded that the piles have only minimal residual load, if any. The strain gage readings at the start of the static loading tests were considered to be true zero values.

### 7.2 Measurements of Strain during the Static Loading Tests on Piles TP1 through TP3

The purpose of strain gage instrumentation is to establish the load distribution in the pile during the static test. In principle, this is simple to obtain by multiplying the measured strain with the pile area, A, and modulus, E. In the subject study, however, neither the area nor the modulus were accurately known. As indicated above, the pile diameter and, therefore, the area varied along the pile. Moreover, concrete modulus is not a constant but reduces with increasing strain. As developed by Fellenius (1989, 2014), the modulus, E, or the pile stiffness, EA, can be determined directly from the load-strain data. For a gage located where no or only minimal shaft resistance develops between the pile head and the gage level, the condition for the uppermost gage level location, the secant stiffness can be determined from the relation $Q/\varepsilon$ vs. $\varepsilon$, where Q is the applied load and $\varepsilon$ is the measured strain. At gage levels deeper down the pile, the incremental stiffness relation can be determined from the relation $(Q_2-Q_1)/(\varepsilon_2 - \varepsilon_1)$ vs. $\varepsilon$, which relation also determines the secant stiffness relation to use in the analysis of the test data. The first condition for the incremental method to work is that the load movement response of the test pile is representative for the ultimate shaft shear response. The second condition is that the ultimate shaft shear exhibits no significant strain hardening or strain softening. The third is that the data must be accurate both with regard to load and strain (as the method applies differentiation, small errors or imprecisions will be amplified in the results).

Figure 12 shows the secant stiffness versus strain in Pile TP1, a standard bored pile, for the uppermost gage level, GL6, located at 1.0 m depth. Linear regression of the secant stiffness vs. strain established the indicated secant stiffness of the pile. The correlation coefficient (0.8807) is somewhat low but acceptable. Figure 13 shows the incremental stiffness for the same gage level. The differentiation has accentuated the small errors and variations, the correlation is not good. The test was not carried far enough to make possible incremental stiffness evaluation for the other gage levels.

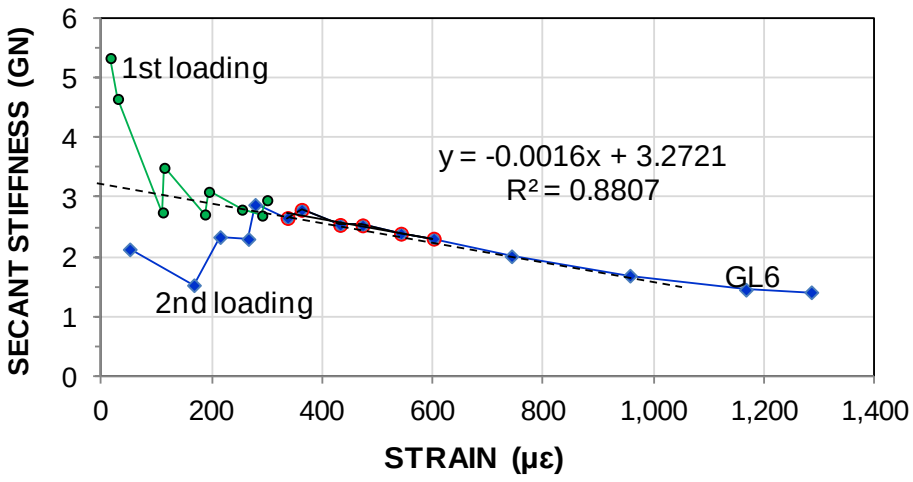


Fig. 12 Pile TP1 Secant stiffness for the uppermost gage level, GL6

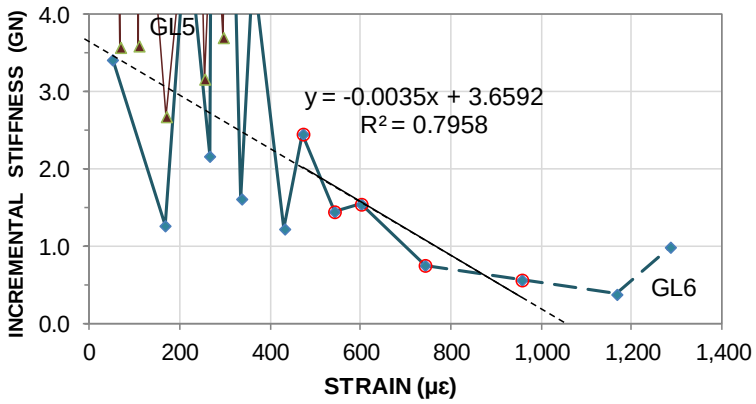


Fig. 13 Pile TP1 Incremental stiffness for the uppermost gage levels, GL6 and GL5

The relevance of the secant stiffness relation determined from the incremental stiffness method is shown in Figure 14 where the applied loads are plotted versus the measured strains for all six gage levels. There is a good agreement between the measured loads and the loads calculated from the strains using the secant stiffness relations.

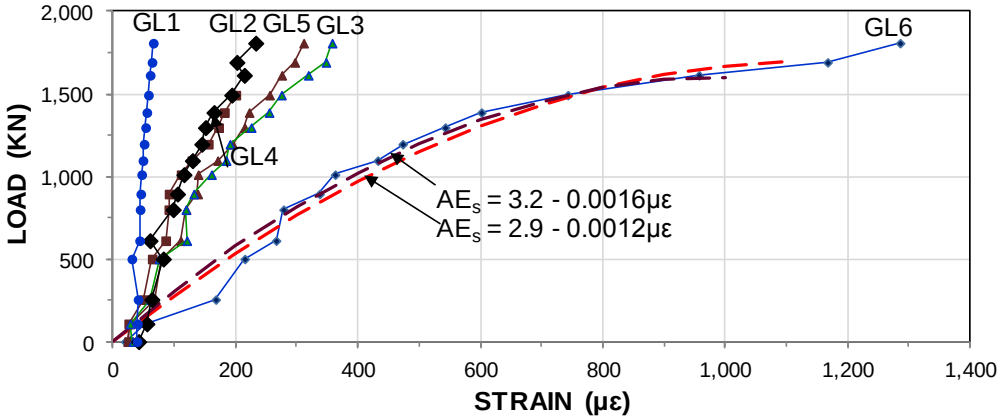


Fig. 14 Pile TP1 Load-strain records

Figure 14 also indicates that Gage Level GL6 response was much softer (the slope is flatter) than the other gage levels. Moreover, the relation for Gage Level GL3 was a bit softer than that of Gage Levels GL5 and GL4. These difference in softness (slope) of the load-strain curve is a sign of differences in pile cross sectional areas between the gage levels.

The same analysis approach was applied to the records of the FDP pile, Pile TP2 and the response was similar to that found in Pile TP1. The strain-gage records from gage levels GL2, GL3, and GL4 in Pile TP3, FDP Pile with Expander Body, turned out to be somewhat erratic and unreliable, and the range of strain developed in the test did not allow for pile stiffness estimation. Because the tests were not carried to anywhere near the intended maximum loads, only a few secant stiffnesses could be determined from the strain-records, as presented in Table 1.

**TABLE 1 Secant Stiffness Relations**

| | | | |
|---|---|---|---|
| TP1 GL1 | AE$_s$ = 3.7 - 0.002με | TP4 GL1 | AE$_s$ = 3.8 - 0.002με |
| | | TP4 GL2 | AE$_s$ = 4.4 - 0.002με |
| TP2 GL5 | AE$_s$ = 3.1 - 0.001με | TP4 GL4 | AE$_s$ = 4.4 - 0.002με |
| TP2 GL4 | AE$_s$ = 3.8 - 0.001με | TP4 GL5 | AE$_s$ = 4.4 - 0.002με |

### 7.3 Measurements of Strain during the Static Loading Tests on Piles TP4

Figure 15 shows the strains measured in Pile TP4. Gage Level GL6 ceased to provide meaningful data at the end of Phase 1, but the other gage levels worked well throughout. At the end of the first bidirectional-cell test (Phase 1), no significant strain remained in gage levels GL2 through GL5 above the cell, as opposed to GL1, located below the cell and above the EB, where about 100 με of compression remained after the cell had been unloaded. During Phase 2, the head-down test, the cell was kept draining in the response to the downward movement of the shaft. That is, the cell recorded no load. It is therefore remarkable that gage level GL1 yet recorded strain. It would appear that the shaft resistance above the cell imposed loads and downward soil movement below the cell, conveying load onto the shaft between the cell and the EB. However, we believe that a more plausible reason is that during Phase 1 the surrounding sand and gravel entered the opening between the upward moving pile portion and the downward moving lower portion, due to it being drawn-in by the sucking action associated with the opening between the cell plates. This soil created an unknown amount of resistance to the Phase 2 closing of the opening, which resulted in the force measured in GL1 during Phase 2 test.

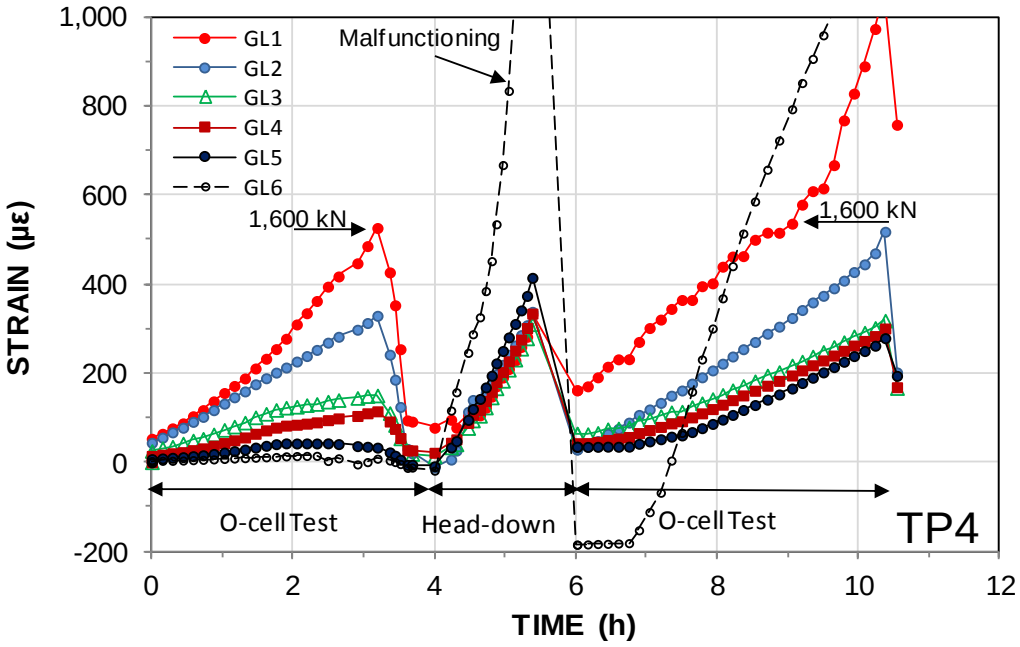


Fig. 15 Pile TP4 Strain versus time for Phases 1 through 3. GL6 malfunctions

The incremental stiffness relations determined from the TP1, TP2, and TP4 tests are shown in Table 1 above. The stiffness values are very approximate and a small change of the selection of data points to use for the regression will change the evaluated stiffness values considerably. It is clear however, the stiffness is very much dependent of the strain. The difference in initial stiffness, ranging from 3.1 through 4.4 GN reflects that the pile diameter varies in the piles—there are bulges and neckings. The range 3.1 through 4.4 GN in Pile TP4 corresponds to a relative increase of about -9 % through +9 % or about 40 mm of a 450-mm average pile diameter.

### 7.4 Load Distributions Calculated from the Strain Measurements

**Test Piles TP1 - TP3**. Figures 16 and 17 show the calculated load distributions for the head-down tests on Piles TP1 through TP3. The loads have been calculated using the secant stiffness relations indicated in the figures. The selection of stiffness relation for the gages that were not determined from the analyses were assumed to be the same as those that were found in the analysis of adjacent gage levels. However, when a calculated range of loads differed from what appeared to be reasonable

distribution, the value that gave a more reasonable distribution won out. It is obvious that for these test piles, the stiffness relations are very approximate. The main results was that they have provided a general even distribution from the pile head to the pile toe and assisted in determining the approximate toe response mobilized in the tests. The addition of the EB to Pile TP3 resulted in a significant increase of toe resistance.

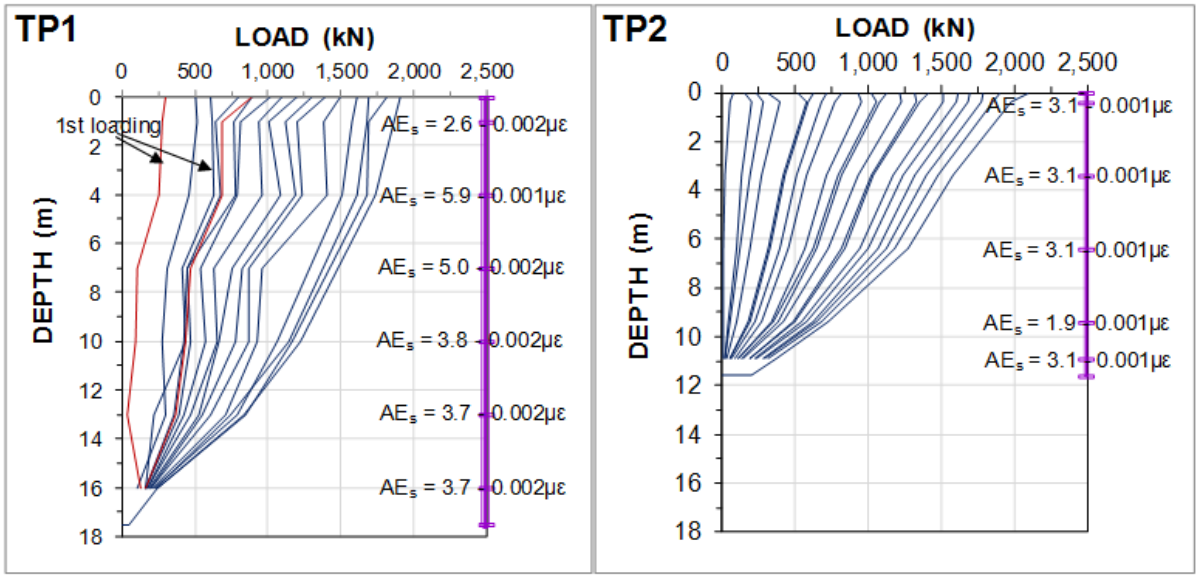


Fig. 16 Piles TP1 and TP2 Load distributions and applied stiffness relations

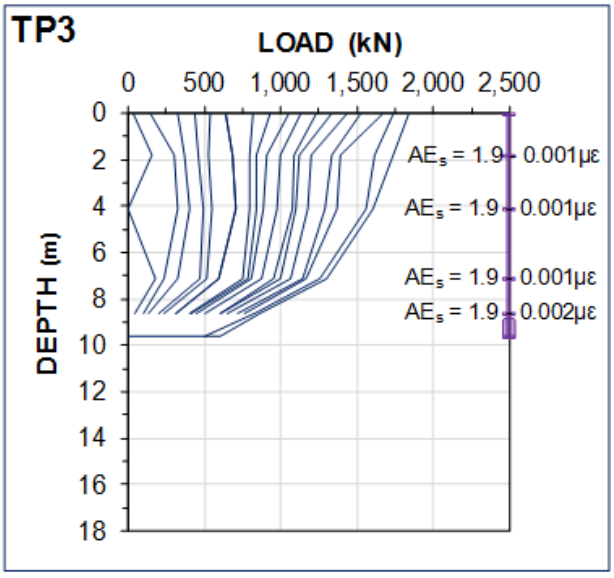


Fig. 17 Pile TP3 Load distribution and applied stiffness relations

**Test Pile TP4 Phase 1**. Figure 18 shows the load distributions for the bidirectional-cell test, similarly calculated. Figure 19 shows the equivalent head-down load distributions which is constructed by "flipping" or mirroring the measured distributions to model the same loads and resistances for an equivalent head-down test. As indicated, the "flipped" distribution indicates a maximum load of about 3,300 kN for the same loads at the cell level and pile toe. Even if the pile had been constructed with a stronger material, it is not likely that a head-down test could have successfully loaded the pile to the large load indicated. N.B., the downward cell movement was a mere 3 mm in the test. Obviously, much additional resistance could have been mobilized by the EB.

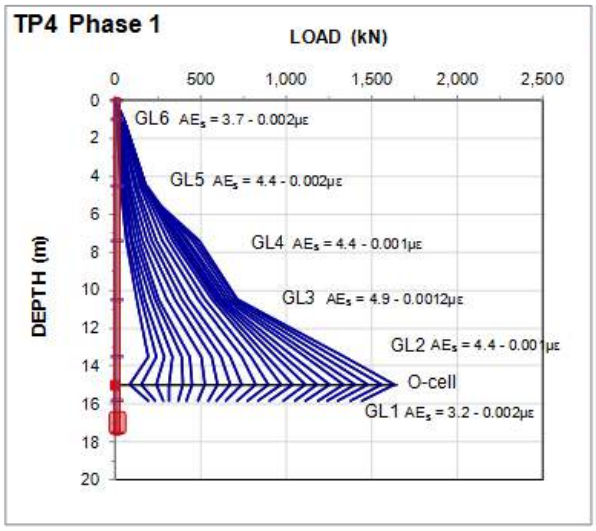


Fig. 18 Pile TP4Phase 1 Load distribution and applied stiffness relations

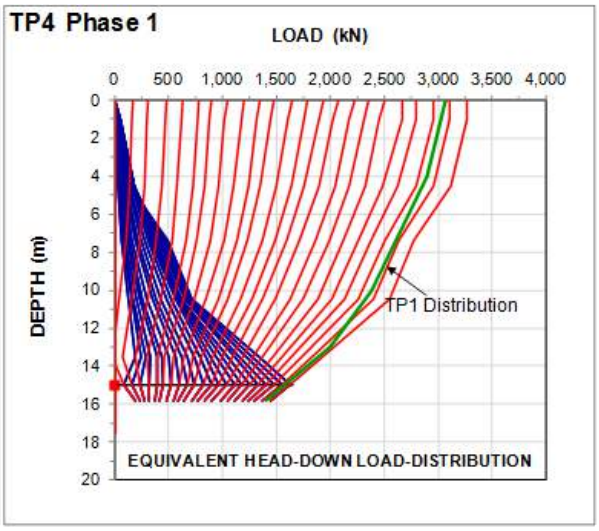


Fig. 19 Pile TP4 Phase 1 Equivalent head-down load distribution

**Test Pile TP4 Phase 2**. Figure 20 shows the measured loads during Phase 2, the head-down test. As shown, Gage Level GL1, below the cell registered significant load, despite the fact that the cell was kept free-draining and unloaded. We believe that the surrounding soil (sand and gravel) was "sucked" into the opening between the cell plates in Phase 1. This soil then provided resistance to the Phase 2 closing of the opening. The load distribution data are not useful for soil analysis.

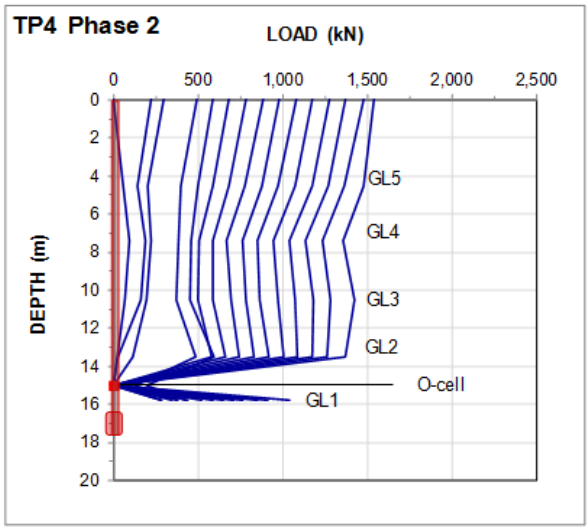


Fig. 20 Pile TP4 Phase 2 Load distribution

**Test Pile TP4 Phase 3**. Figure 21 shows the measured loads during Phase 3, the repeat bidirectional-cell test. The load distribution calculated for the maximum load in the Phase 1 test is added. The distributions for the maximum load above the cell in the two test phases are very different. The downward cell load and the EB response are quite similar, however. The soil response to the push-up, push-down, and push-up again appears to have resulted in a weakening of the soil layers above GL3 that was offset by a strengthening below GL3. At first glance, comparing the distributions at maximum load for Phases 1 and 2, it would seem as if Phase 1 would be affected by residual load that had been removed (released) from Phase 3. However, this begs the question, where are the strain changes that represent the removal? All load values are in reference to the same start ("zero") value. Possibly, the Phase 3 reloading caused a released of residual strain as the load was increased.

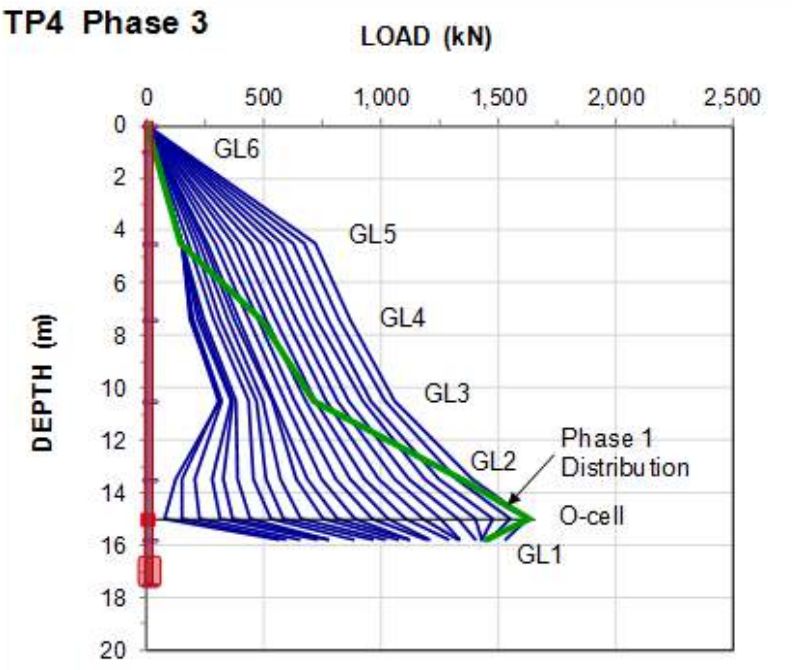


Fig. 21 Pile TP4 Phase 3 Load distribution

However, the strain-gage records during the wait period indicate that no significant residual load developed in the piles prior to the start of the static loading tests. Unfortunately, the accuracy of the strain responses is not sufficiently trustworthy to allow much conclusions in this regard.

Figure 22 compiles the load distribution for the maximum applied load in the four tests showing that:

1. The standard piles, Piles TP1 and TP4, mobilized the shaft resistance equally.

2. The two FDP piles, Piles TP2 and TP3, showed very similar shaft response. Despite having a smaller diameter, the FDP piles mobilized more than twice as much shaft resistance (per unit length) as the standard pile.

3. The very similar measured shaft resistance distributions for Piles TP1 and TP4 and for Piles TP2 and TP3 were fitted to an effective stress analysis. The fitted distribution is shown by black dashed curves in the figure.

4. The CPTU records were used to calculate the shaft resistance distribution applying the Eslami-Fellenius CPTU-method (Eslami and Fellenius 1997) to the 12.5 m sounding depth. The CPTU-calculated distribution is shown by purple dashed curves in the figure. The agreement between the measured distributions and the CPTU-determined distribution is remarkable. However, it is probably also somewhat coincidental.

5. The addition of the EB to Pile TP4 added significant toe resistance to Pile TP4.

6. It is quite obvious from the overall test data that neither of tests on Piles TP1 through TP3 significantly engaged any toe resistance, EB or no EB.

The effective stress analysis fit to the load distributions were made using the UniPile software (Goudreault and Fellenius 2013). The CPTU calculation of shaft resistance was made from the CPTU records using the UniPile software.

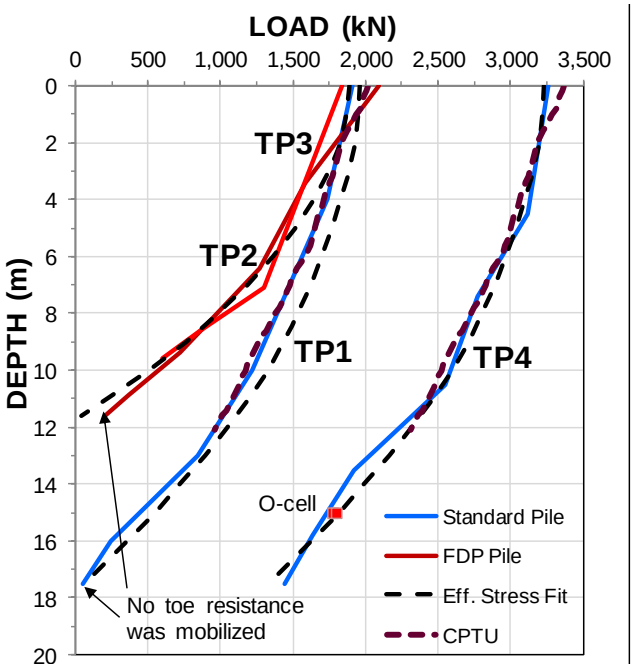


Fig. 22 Compilations of the load distribution at maximum load

It is recognized that the loads obtained from the strain gage data and stiffness evaluations were approximate. However, the shaft resistance above 15.0 m depth was measured separately for Pile TP4 (Phase 1, the bidirectional-cell test). Therefore, the shaft resistance distribution of for Piles TP1 and TP4 is considered representative for the shaft response of the standard pile at the site.

The load distributions for Piles TP2 and TP3 also shown in the figure, are based on the same reasonable assumption that no appreciable load reached the pile toe in the tests in contrast to Pile TP4. For Pile TP4, the bidirectional cell provided a toe load of approximately 1,500 kN which resulted in only 3 mm of movement of the EB equipped pile toe.

The effective stress calculations for fitting a calculated load distribution (shaft resistance) to the measured distributions assumed one upper 10 m thick layer deposited on a lower, slightly denser layer. The input of soil density values and location of the groundwater table was taken from the soil profile of the site. For Piles TP1 and TP4, the fit was obtained with beta-coefficients of 0.5 and 0.6 for the upper layer and lower layers, respectively. For Piles TP2 and TP3, the fit was obtained applying a beta-coefficient of 0.5 at the upper boundary of the upper layer, increasing linearly to 1.4 at the lower boundary. In the lower layer, it was assumed to be 1.4.

## 8. RESULTS OF DYNAMIC TESTS

Three months after the static tests, all four piles were subjected to impacts from a 3,880-kg drop hammer. The driving was monitored with the Pile Driving Analyzer, PDA, and the records were analyzed using the CAPWAP software from GRL. The CAPWAP analysis produces, amongst other information, a static resistance and its distribution in the pile. Provided that the pile moves a sufficient distance for the blow and the net pile movement is at least about 3 mm/blow, then, the CAPWAP-determined resistance is considered similar to the pile capacity and used as such in design. If the net movement is smaller, the maximum resistance evaluated by the CAPWAP analysis is usually smaller than the pile capacity and the resistance distribution often less precise. Table 2 compiles the data for the four test piles. For all four piles, the net movement was smaller than the ideal value. Therefore, the calculated shaft resistance in the lower portion of the pile and the toe resistance was probably smaller than the actual resistance, i.e., the CAPWAP-determined capacity was smaller than the actual. Figure 23 shows the CAPWAP-determined load distributions.

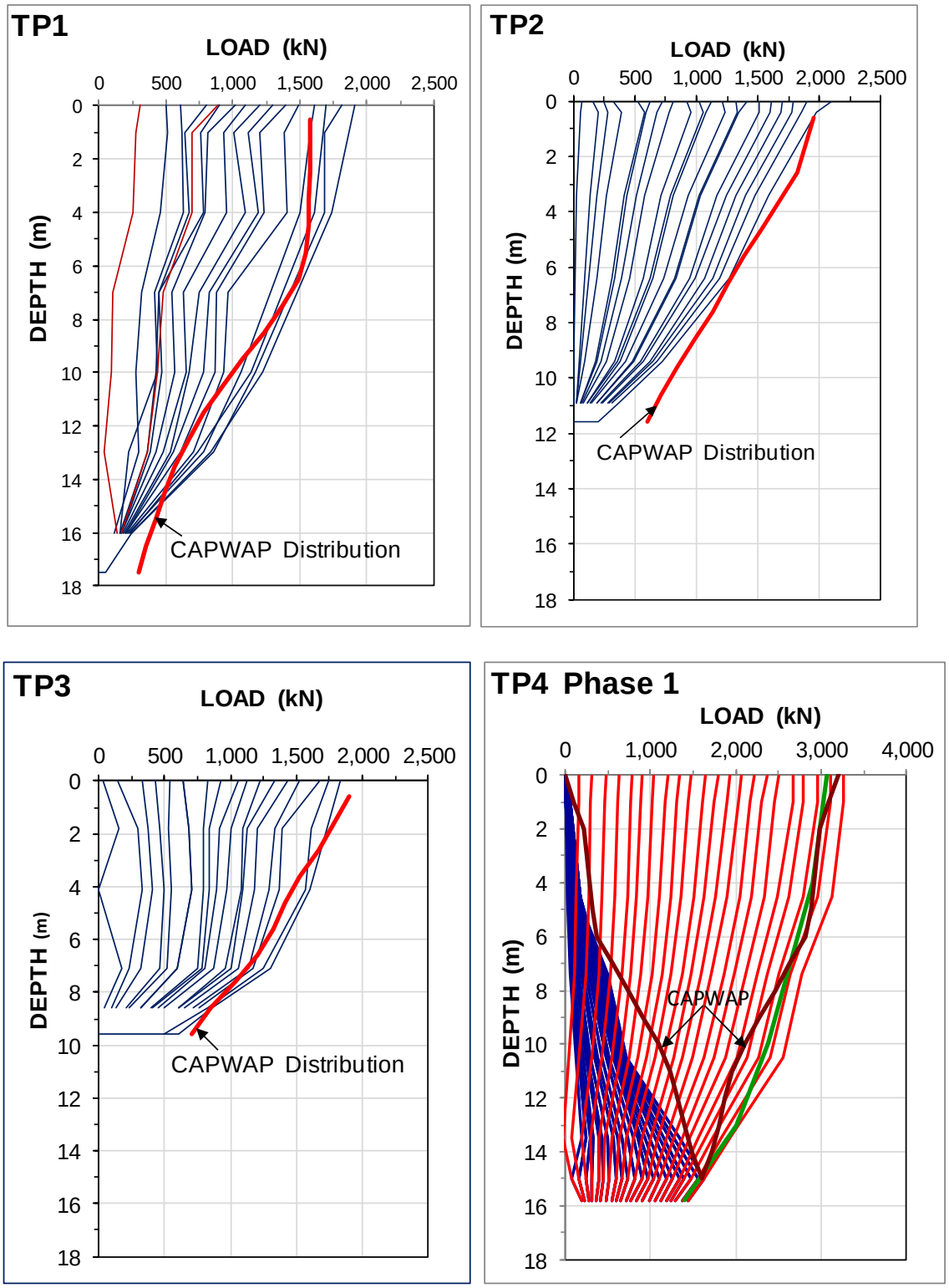


Fig. 23 The CAPWAP-determined static load distributions compared to the distributions evaluated in the static loading tests. The TP4 diagram includes both the upward distributions and the equivalent head-down distributions.

The toe resistance showed for Pile TP4 originated from viscous resistance in the water in between the bidirectional-cell plates could not be squeezed out fast enough through 15 m long , 6-mm hose connecting the void inside the cell to the ground surface to the activating hydraulics (now removed).

**TABLE 2 Pile Driving Observations and CAPWAP Results**

| Pile (#) | Drop height (m) | net mvmnt (mm/bl) | quake toe | gross toe (mm) | Equivalent toe movement (bl/m) | (bl/25mm) | Shaft and Toe Resistance (kN) | (kN) |
|---|---|---|---|---|---|---|---|---|
| TP1 | 0.8 | 1.5 | 3 | 3.4 | 700 | 17 | 1,300 | 300 |
| TP2 | 1.0 | 1.0 | 5 | 5.4 | 700 | 17 | 1,200 | 700 |
| TP3 | 0.8 | 1.0 | 5 | 4.8 | 1,000 | 25 | 1,100 | 850 |
| TP4 | 0.8 | 2.0 | 7 | 8.5 | 500 | 13 | 1,300 | 250 |

Coincidentally, the maximum load applied to Pile TP1, TP2, and TP3 was about the same as the maximum CAPWAP-determined resistances in the dynamic tests. The slope of the load distributions for the two types of tests were reasonably similar considering the uncertainties of the loads determined from the strain gage records and the fact that the resistances were not fully mobilized in the dynamic tests on Pile TP1, TP2, and TP3. The CAPWAP-determined load distribution for pile TP4 is plotted both as shaft resistance and as resistance rising from the cell load. The TP4 maximum shaft resistance is considered to represent the ultimate resistance for both test types.

If the TP4 distributions are taken at face value, the static Phase 1 distribution suggests presence of residual load, which was more or less removed in the Phase 4 test, causing the CAPWAP-determined distribution to be closer to the actual shaft resistance. That is, the difference between the two distributions could be due to the residual load. However, this is hypothetical only and the difference could also be due to the uncertainties of both measurements.

The static loading test on Pile TP4, mobilized the shaft resistance of the length above the bidirectional-cell test. Figure 24 shows the load-movement curve of the upward portion of the cell test plotted as load vs. movement. The CAPWAP-determined shaft resistance has been added to the diagram starting from the total movement at the end of Phase 3. The important point is that the CAPWAP-determined shaft capacity agrees with that found in the static loading test. The stiffer response of the CAPWAP curve for the latter half of the test, as opposed to the static test curve, could be an effect of the reloading condition.

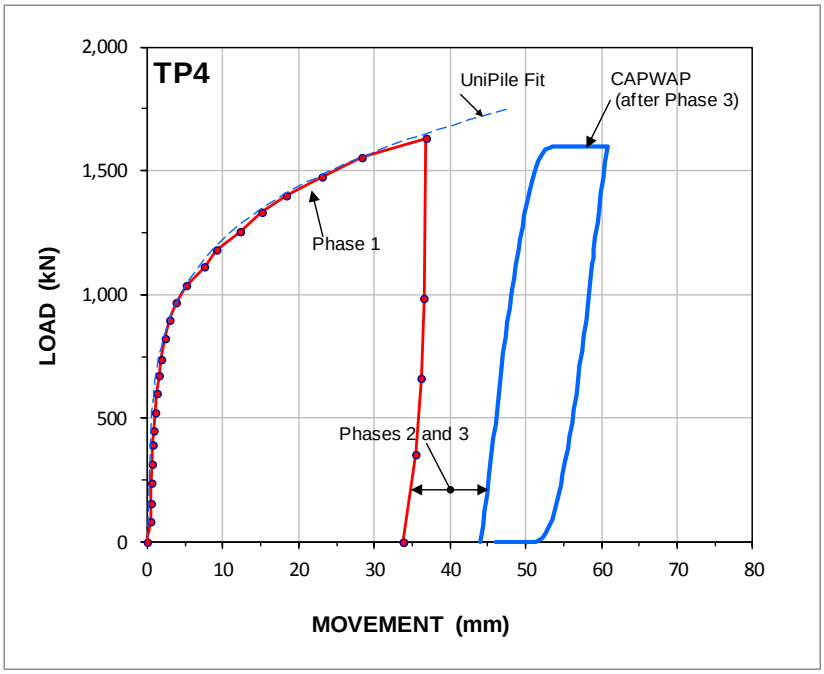


Fig. 24 Shaft resistance load-movement curve from the static loading test on Pile TP4 and that determined in the CAPWAP analysis

## CONCLUSIONS

Despite the unplanned somewhat premature termination of the head-down tests on Piles TP1, TP2, and TP3, informative data were obtained from these tests. The successful bidirectional-cell test on Pile TP4 provided very useful data which also enhanced the results of the head-down tests.

The beta-coefficients of 0.5 and 0.6 evaluated from the results on the standard bored pile showed the local soils to be quite competent for a compact silty sandy soil. However, the displacement compaction achieved by the Full Displacement Pile, FDP, showed to improve the shaft resistance considerably, increasing the beta coefficient from 2 to 3 times that of the standard pile.

The addition of the EB showed to have greatly enhanced the stiffness response of the pile toe.
Understandably, the predictions of capacity showed a considerable scatter. The large scatter of also the movements at the various capacity values is more surprising. It gives reason for concern regarding the uniformity of the methods of evaluating capacity from a static loading test currently applied by the practice.

The ultimate shaft resistance of Pile TP4 was mobilized in both the static test and the dynamic and the values from the two test methods agreed well with each other. The load distributions evaluated from the measured strains and the CAPWAP-determined distributions agreed reasonably well with each other.

## ACKNOWLEDGEMENTS

We are most grateful for the indispensable contribution provided to the study by Fugro Loadtest, who supplied all materials and performed the Osterberg-cell test at no charge to the project.

We very much appreciate the contribution from Mr. Hicham Salem of AATech International Inc. in setting up the instrumentation of Piles TP1 through TP3, assistance in compiling the raw data, as well as performing the CAPWAP.

We are also thankful for the contribution from Pile Dynamics, Cleveland, who supplied the thermal wires for the instrumentation free of charge.

## REFERENCES

Broms, B.B. and Nord, B, 1985. Axial bearing capacity of the Expander Body pile. Soils and Foundations, Japanese Society of Soil Mechanics and Foundation Engineering, 25(2) 31-44.

Decourt, L., 2008. Loading tests: interpretation and prediction of their results. ASCE GeoInstitute Geo-Congress New Orleans, March 9-12, "Honoring John Schmertmann—From Research to Practice in Geotechnical Engineering", Geotechnical Special Publication, GSP 180, Edited by J.E. Laier, D.K. Crapps, and M.H. Hussein, pp. 452-488.

Eslami, A. and Fellenius, B.H., 1997. Pile capacity by direct CPT and CPTU methods applied to 102 case histories. Canadian Geotechnical Journal 34(6) 886–904.

Fellenius, B.H., 1989. Tangent modulus of piles determined from strain data. The ASCE Geotechnical Engineering Division, 1989 Foundation Congress, Edited by F.H. Kulhawy, Vol. 1, pp. 500-510.

Fellenius, B.H., 2114. Basics of foundation design. Electronic Edition. www.Fellenius.net, 428 p.

Fellenius, B.H., Kim, S.R., and Chung, S.G., 2009. Long-term monitoring of strain in instrumented piles. ASCE Journal of Geotechnical and Geoenvironmental Engineering, 135(11) 1583-1595.

Goudreault, A.A and Fellenius, B.H., 2013. UniPile Version 5, Users and Examples Manual. UniSoft Geotechnical Solutions Ltd. [www.UniSoftLtd.com]. 100 p.

Massarsch, K.R. and Wetterling, S., 1993. Improvement of augercast pile performance by Expander Body system. 2nd International Seminar on Deep Foundations on Bored and Auger Piles, Ghent, June 1 - 4, 1993, pp. 417-428.

Mullins, G. Thermal integrity profiling of drilled shafts. DFI Journal 4(2) 54-64.

Terceros Herrera, M., Wetterling, S. and Massarsch K. R. 1995. Application of the Soilex Pile System with Expander Body in Bolivia. Proc. of 10th. Congreso Panamericano de Mecánica de Suelos e Ingeniería de Cimentaciones. Guadalajara, Mexico, pp. 1319-1327.